Plasma Formation and Implosion Structure in Wire Array *Z* Pinches

J. P. Chittenden, S. V. Lebedev, A. R. Bell, R. Aliaga-Rossel, S. N. Bland, and M. G. Haines
The Blackett Laboratory, Imperial College, London SW7 2BZ, United Kingdom
(Received 19 March 1999)

The transformation of a cylindrical array of metallic wires into an imploding *Z*-pinch plasma is described using a 2D resistive magnetohydrodynamics code. The persistence of unionized wire cores dominates the collapse structure. Low-density coronal plasma is swept around the wire cores generating radial plasma streams which reach the axis forming a precursor plasma at roughly half the implosion time. The final stagnation comprises high-density plasma streams impacting onto this precursor. Azimuthal modulation of the plasma is retained throughout. The code accurately reproduces a number of features of experiments with 1 MA currents and predicts qualitatively similar results for higher currents.

PACS numbers: 52.55.Ez, 52.58.Ns, 52.65.Kj

Wire array *Z* pinches are the world's most powerful laboratory x-ray sources. In experiments at Sandia National Laboratories, cylindrical arrays of up to 400 fine tungsten wires are imploded by a 20 MA current pulse, producing a transient hot dense plasma which emits 2 MJ of x rays with a peak power of 290 TW [1,2] (in a nested array configuration [3]). Such x-ray pulses can be used to energize hohlraums for either inertial confinement fusion research or other high energy density applications. The spectacular improvements in x-ray power attained in the last couple of years are directly attributable to the improved symmetry and stability of implosion obtained with wire arrays. Recent experiments [4] have clearly demonstrated that increasing the number of wires in the array, increases the x-ray power obtained. This trend is generally ascribed to higher wire number experiments better approximating a uniform plasma shell. Recent experiments [5,6], however, using arrays of 8–64 15-μm aluminum wires driven by the MAGPIE generator [7] show no evidence of shell formation and indicate that implosion is a complex three-dimensional (3D) process. Radial streams of plasma emanating from the wires are observed to reach the axis forming a precursor plasma at roughly half the final implosion time. The majority of the array's mass is, however, retained in the high-density wire cores until late in the implosion. Superimposed on this azimuthal asymmetry are both uncorrelated $m = 0$ like instabilities, local to the individual wire plasmas, and a global Rayleigh-Taylor instability during the final implosion.

In this Letter, we describe how the radial and azimuthal structure of the plasma in these experiments results from the slow rate of wire ablation and the topology of the magnetic field. "Cold-start" calculations are used to show how the initial explosion of each wire results in a high-density wire core surrounded by a low-density corona. These results then provide the initial conditions for 2D (x, y) simulations which show how the coronas are swept around the wire cores forming the radial plasma streams and the precursor. The plasma structure during the final implosion phase is found to be substantially different from that obtained in cylindrical shell implosions.

A 3D resistive magnetohydrodynamic (MHD) code has been developed to model wire array *Z*-pinch experiments. Three-dimensional runs with adequate spatial resolution would require far greater computational resources than are presently available to the authors. In this Letter, we present results obtained using this code limited to two dimensions in the x-y (or r-θ) plane. The code evolved from an ideal MHD code used to model galactic jet formation [8]. Explicit hydrodynamics is performed on a Cartesian (x, y, z) Eulerian grid with cubic cells, using second order Van-Leer advection. The thermal and magnetic field diffusion equations are solved implicitly by the iterative solution of matrix equations. The model is two temperature (electrons and ions) with local thermodynamic equilibrium ionization and a simple radiation loss model [9].

The 100 μm cell size adopted for these calculations does not allow the initial breakdown and ionization phase of the individual wires to be resolved. We therefore begin by modeling the early behavior of a single wire using 1D (r) and 2D (r, z) cold-start simulations with 2.5 μm spatial resolution. The results of these calculations are then used as the initial conditions for 2D (x, y) simulations of the whole array. A similar cold-start model to Ref. [10] is used with the addition of a Thomas-Fermi equation of state and Lee and More's transport coefficients [11] which allow the phase transitions from solid to plasma to be approximated. A prescribed current waveform is applied to the problem. More formally, one should calculate the mutual inductance between array wires and the self-consistent currents obtained for a prescribed voltage [3].

For the 15 μm aluminum wires used in MAGPIE experiments [5,6] uniform vaporization occurs at around 300 A per wire. As the wire material expands, the density of the surface region drops sufficiently for ionization to occur, forming a plasma corona. As the current begins to flow in the coronal plasma, it is rapidly heated to $\sim$10 eV and expands at the corresponding ion sound speed ($\sim 10^4$ m s^{-1}). At $\sim$2 kA per wire, the magnetic field becomes sufficient to confine the coronal plasma, rapid expansion ceases, and quasistatic conditions ensue.

 0031-9007/99/83(1)/100(4)$15.00 © 1999 The American Physical Society

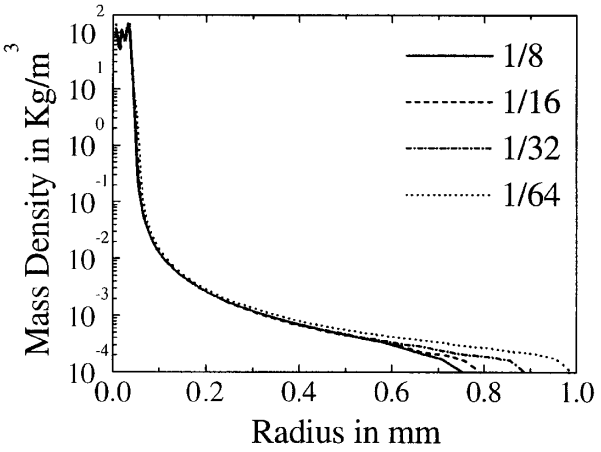

FIG. 1. Mass density profiles from 1D cold-start simulations of 15 μm aluminum wires.

Figure 1 shows radial density profiles from 1D cold-start simulations of 15 μm aluminum wires carrying $\frac{1}{8}$, $\frac{1}{16}$, $\frac{1}{32}$, and $\frac{1}{64}$ of the MAGPIE current (1 MA peak current, 240 ns 0%–100% rise time). Each profile is shown at 3 kA per wire, i.e., rather 24, 34, 48, and 69 ns, respectively. The remarkable similarity of these curves suggests that in this situation the structure of individual wire plasmas is determined by the absolute value of the current and is insensitive to the time taken to reach that current. In each case, 99% of the wire mass remains in the high-density, unionized, cold core with 99% of the current flowing in the corona. Further ablation of the core relies upon thermal conduction of energy from the hotter corona and is relatively slow. The cold core therefore persists, in 1D calculations, until well after the peak current.

Once the rapid circular expansion of the corona ceases, the shape of the plasma in the x-y plane is determined by the topology of the magnetic field and, in particular, the ratio of the local field generated by the current in each wire plasma ($\mathbf{B}_{\mathrm{local}}$) to the global field of the entire array ($\mathbf{B}_{\mathrm{global}}$). The cold-start calculations of 15 μm aluminum wires are therefore terminated when the current reaches 3 kA per wire and the generic results illustrated in Fig. 1 used as the initial conditions for 2D (x, y) simulations of the entire array. The 100 μm resolution used in 2D (x, y) calculations mean that the residual cold cores are initially represented by single cells of neutral gas. This appears to be a fair approximation since cold-start calculations show that for currents greater than 3 kA the core is a uniform density and temperature object, carrying little current and slowly expanding to become a neutral gas. While 2D (r, z) cold-start calculations indicate the development of $m = 0$ instabilities in the individual wires much later in the discharge, the perturbation amplitude was negligible at the time when 2D (x, y) calculations were initiated.

Figure 2 shows a progression of logarithmic mass density contours from a 2D (x, y) simulation of a 16 mm diameter array of eight 15-μm aluminum wires driven by the MAGPIE generator. One-quarter of the full array is simulated with reflective boundary conditions.

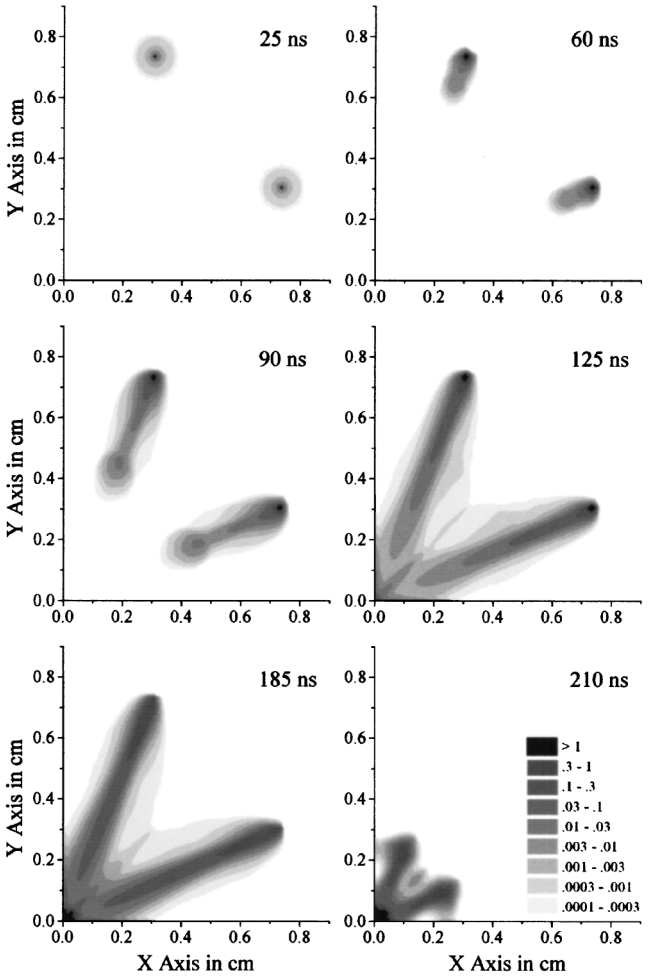

FIG. 2. A progression of mass density contours from a 2D (x, y) simulation of eight 15-μm aluminum wires on MAGPIE.

At 60 ns, the coronal plasma has been significantly deformed by the global magnetic field of the array. Pinching of the corona on the azimuthal sides and outward radial side of the wire improves the coupling of thermal energy to the core and accelerates the rate of core ablation. The release of material from the core increases the pressure of the corona which then expands in the direction of least resistance, i.e., in the negative radial direction, into the low magnetic field region inside the array. The experimentally determined delay between the start of the current and observable activity in the wire plasmas (often referred to as the dwell time) appears to correspond to the time taken to pinch the corona and initiate faster core ablation.

While the absence of current in the neutral wire cores and their high mass density mean that at this stage they remain virtually unmoved, any further material liberated from the wire cores into the low-density corona experiences rapid acceleration by the $\mathbf{j} \times \mathbf{B}_{\mathrm{global}}$ force towards the array axis. As a consequence, the plasma

coronas are swept around the wire cores giving rise to radial streams of plasma.

The plasma in the streams is kept cool, primarily by ionization energy losses and to a lesser extent by radiative cooling, and maintains roughly constant 10–20 eV electron and ion temperatures. The average radial velocity of plasma in the stream is $\sim 10^5\ \mathrm{m\,s^{-1}}$, i.e., 5 times the local ion sound speed. At the edges of the stream where the density is lowest and the acceleration highest, the radial velocity reaches $1.8 \times 10^5\ \mathrm{m\,s^{-1}}$. Since the magnetic field is partially "frozen" into the plasma, the radial streams bring the current inside the array radius. While the current density is maximum in the plasma surrounding the wire cores, it remains finite throughout the plasma stream. Both the high Mach number of the flow and the presence of finite azimuthal $\mathbf{j} \times \mathbf{B}$ forces serve to collimate the radial plasma stream throughout the implosion. Penetration of the current inside the array is reduced in calculations with more wires and hence smaller interwire gaps and better screening. As an example, 41% of the current flows within 6 mm of the axis for 8 wires at 125 ns; this figure drops to 32% for 16 wires and 24% for 32 wires.

The radial streams of plasma first interact with one another at 105 ns at a radius of 2.5 mm. 10 ns later, at roughly half the final implosion time, the first plasma arrives on the axis. The density contour map at 125 ns illustrates the structure of the "precursor" pinch formed on the axis. Low-density material pervades the region within the interaction radius; however, this material retains it's radial velocity and converges to the axis to form a high-density, high temperature central region of $\sim 500\ \mu\mathrm{m}$ diameter. At precursor formation, 55% of the array mass remains in the wire cores with 15% in the dense plasma immediately surrounding them and the remainder in the radial streams.

From this point onwards, the implosion of the array is a continuous process. The wire cores are gradually depleted as they ablate more coronal material which is rapidly accelerated towards the accreting precursor plasma on axis. Figure 3 shows the fraction of mass in the wire cores and in the precursor on axis as functions of time. The gradual increase in precursor mass is accompanied by an increase in the current transferred to the precursor. However, it is the inertia of the radial plasma streams which confines the precursor and maintains a roughly constant 40 eV temperature rather than magnetic confinement and Ohmic heating since less than 10% of the total of the current is transferred.

By 175 ns the wire cores have fully ablated, generating a high-density plasma from 6 to 8 mm radius containing 40% of the array mass. The final implosion of this mass is very rapid and generates the substantial kinetic energy which is responsible for x-ray production at the final stagnation.

The mass density contour map at 210 ns shows the pinch structure just prior to final stagnation. In cylindrical shell implosions (in the absence of instabilities) one would expect 100% of the mass to reach the axis almost simultaneously with a final collapse velocity of $\sim 3 \times 10^5\ \mathrm{m\,s^{-1}}$. By contrast, the final collapse stage of an eight wire array is comprised of azimuthally discrete radial plasma streams containing 40% of the mass impacting at $4.5 \times 10^5\ \mathrm{m\,s^{-1}}$ onto a precursor containing 60% of the mass. The reduced mass and increased velocity of the final implosion result in similar kinetic energy and x-ray yield to that of a cylindrical shell. In experiments, the degree of plasma compression at stagnation and the consequent radiation pulse width are dominated by the development of three-dimensional Rayleigh-Taylor instabilities. In the absence of these effects, the code predicts very tight compression to ~ 0.25 mm radius and a short 2 ns radiation burst.

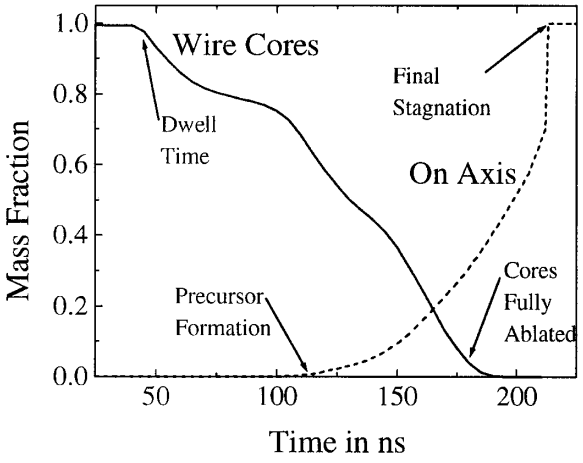

FIG. 3. The fraction of mass in the wire cores and precursor as functions of time.

Quantitative comparisons of these results with experimental data [5,6] indicate accurate agreement for a number of key parameters. The time of the first observable expansion of the wire corona (the dwell time), the inward radial, azimuthal and outward radial velocities, the timing of the first plasma on axis, the time of the first x-ray emission from the precursor, and the time of final implosion are all in agreement to within 10%. The electron number density profiles for the plasma around the wires, in the radial streams, and in the precursor are also in close agreement.

Simulations of MAGPIE experiments with more than eight wires exhibit qualitatively similar behavior, with wire cores persisting until late in the discharge, and precursor formation at roughly half the final implosion time. However, since the width of the radial plasma streams is insensitive to the number of wires, their first interactions occur at larger radii. The dissipation of kinetic energy in the interaction regions raises the local temperature, lowers the resistivity, and encourages current flow. The result is the formation of secondary plasma streams emanating from the interaction regions, midway between the wires azimuthally. Figure 4 shows a mass density contour map from a simulation of a 32 wire array on MAGPIE.

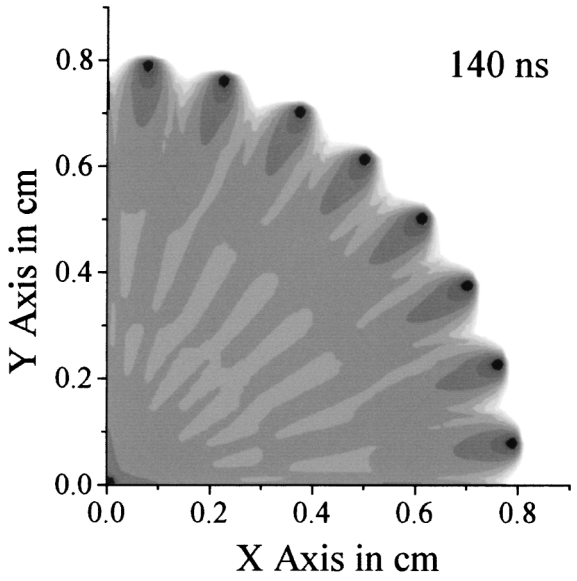

FIG. 4. A mass density contour at 140 ns from a 2D (x, y) simulation of thirty-two 15-μm aluminum wires on MAGPIE.

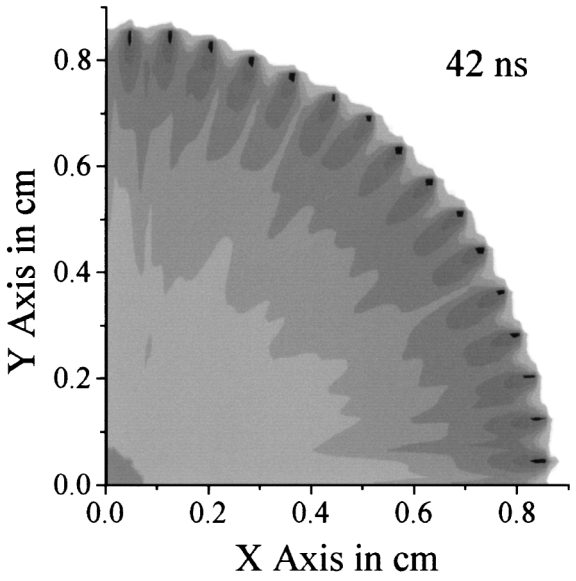

FIG. 5. A mass density contour at 42 ns from a 2D (x, y) simulation of sixty-four 15-μm aluminum wires on SATURN.

Interaction of the primary radial streams emanating from the wires produces secondary streams at 7 mm radius and tertiary streams at 3 mm. This system of coalescing shocks has been observed experimentally using end-on laser schlieren photography [6]. Despite the early merger of the low-density regions, the persistence of wire cores until late in the discharge means both that azimuthal asymmetry is retained throughout the implosion and that 50% of the array mass is in the precursor prior to final implosion.

Qualitatively similar results have also been obtained for experiments on higher current generators with larger numbers of wires, for example, a 17.12 mm diameter array of sixty-four 15-μm aluminum wires on the SATURN generator at Sandia National Laboratories (7 MA peak current, 65 ns 0%–100% rise time). Figure 5 shows a mass density contour at 42 ns, shortly before ablation of the wire cores, showing the strong azimuthal modulation which is retained throughout the implosion. Precursor material is evident on the axis from 30 ns onwards. The shorter time scales of these experiments, however, mean that only 10% of the array mass builds up in the precursor prior to the final implosion when the remaining 90% impacts upon it. The profile of integral mass as a function of radius obtained from Fig. 5 is very similar to the initial profiles used in 1D radiation hydrodynamics simulations [12], where the artificial introduction of precursor material was found to be necessary in order to reproduce the spectral features observed in experiments.

In conclusion we have demonstrated how the ablation of wires and the topology of the magnetic field controls the radial and azimuthal structure of wire array Z-pinch implosions. The accurate reproduction of MAGPIE experiments lends credence to the predictions made for higher current experiments, where detailed data on the implosion structure are not available. In experiments, the results presented here are modulated in the r-z plane both by $m = 0$ instabilities in each wire plasma and by the Rayleigh-Taylor instability in the imploding array as a whole. The absence of these effects means that these calculations cannot explain the observed dependence of x-ray radiation power as a function of the wire number [4]. Where 2D (x, y) calculations are useful is in determining the radial structure prior to final implosion, the degree of azimuthal modulation, and the level of precursor on axis, all of which affect the radiation performance both directly and through their effect on the development of 3D Rayleigh-Taylor instabilities. Determining the fraction of mass in the precursor is particularly important for dynamic hohlraum applications [13], where bombardment of the centrally located foam buffer by radial plasma streams will create significant radiative preheat of any target capsule embedded within it.

This work was supported by the U.K. EPSRC and by the U.S. DoE Contract No. DE-FG03-98DP00217.

[1] G. Yonas, Sci. Am. **279**, No. 2, 40 (1998).
[2] R. B. Spielman *et al.*, Phys. Plasmas **5**, 2105 (1998).
[3] J. Davis *et al.*, Appl. Phys. Lett. **70**, 170 (1997).
[4] T. W. L. Sanford *et al.*, Phys. Plasmas **6**, 2030 (1999).
[5] S. V. Lebedev *et al.*, Phys. Rev. Lett. **81**, 4152 (1998).
[6] S. V. Lebedev *et al.*, Phys. Plasmas **6**, 2016 (1999).
[7] I. H. Mitchell, Rev. Sci. Instrum. **67**, 1533 (1996).
[8] S. G. Lucek and A. R. Bell, Mon. Not. R. Astron. Soc. **281**, 245 (1996).
[9] C. B. Tarter, J. Quant. Spectrosc. Radiat. Transfer **17**, 531 (1977).
[10] J. P. Chittenden *et al.*, Phys. Plasmas **4**, 4309 (1997).
[11] Y. T. Lee and R. M. More, Phys. Fluids **27**, 1273 (1984).
[12] K. Whitney *et al.*, Phys. Rev. E **56**, 3540 (1997).
[13] M. K. Matzen, Phys. Plasmas **4**, 1519 (1997).